Hierarchical Control Scheme for Voltage Harmonics Compensation in an Islanded Droop-Controlled Microgrid

Savaghebi, Mehdi; Guerrero, Josep M.; Jalilian, Alireza ; Vasquez, Juan Carlos; Lee, Tzung-Lin

Published in:
Proceedings of the 9th IEEE International Conference on Power Electronics and Drive Systems, PEDS 2011

Publication date:
2011

Document Version
Early version, also known as pre-print

Hierarchical Control Scheme for Voltage Harmonics Compensation in an Islanded Droop-Controlled Microgrid

Mehdi Savaghebi[1], Josep M. Guerrero[2,3], Alireza Jalilian[1], Juan C. Vasquez[3], and Tzung-Lin Lee[4]
1- Center of Excellence for Power System Automation and Operation, Iran University of Science and Technology
2- Department of Automatic Control and Industrial Informatics, Technical University of Catalonia, Spain
3- Institute of Energy Technology, Aalborg University, Denmark
4- Department of Electrical Engineering, National Sun Yat-sen University, Taiwan
savaghebi@iust.ac.ir, joz@et.aau.dk, jalilian@iust.ac.ir, juq@et.aau.dk, tzunglin.lee@gmail.com

Abstract—**In this paper, a microgrid hierarchical control scheme is proposed which includes primary and secondary control levels. The primary level comprises distributed generators (DGs) local controllers. The local controller mainly consists of active and reactive power controllers, voltage and current controllers, and virtual impedance loop. A novel virtual impedance structure is proposed to achieve proper sharing of non-fundamental power among the microgrid DGs. The secondary level is designed to manage compensation of voltage harmonics at the microgrid load bus (LB) to which the sensitive loads may be connected. Also, restoration of LB voltage amplitude and microgrid frequency to the rated values is directed by the secondary level. These functions are achieved by sending proper control signals to the local controllers. The simulation results show the effectiveness of the proposed control scheme.**

I. INTRODUCTION

MICROGRID is a local grid consisting of Distributed Generators (DGs), energy storage system and dispersed loads and it may operate in both grid-connected or islanded mode [1]. The DGs are often connected to the microgrid through a power electronic interface converter.

The main role of an interface converter is to control power injection. In addition, compensation of power quality problems, such as voltage harmonics can be achieved through proper control strategies. The voltage harmonic compensation approaches of [2]-[5] are based on making the DG unit emulate a resistance at harmonic frequencies.

A method for compensation of voltage harmonics in an islanded microgrid has been presented in [6]. This method is also based on the resistance emulation. Furthermore, a droop characteristic based on DG harmonic reactive power has been considered to achieve sharing of the harmonic compensation effort. As explained in [7] the method of [6] can be modified in order to achieve selective harmonic compensation.

The aforementioned methods are designed for compensation of voltage harmonics at the DG connection point; while, usually the power quality at the load bus (LB) is the main concern; since, the sensitive loads may be connected to it. Thus, in this paper the concept of microgrid hierarchical control [8]-[11] is applied for cooperative compensation of voltage harmonics at the islanded microgrid LB. The compensation is preformed selectively for the main voltage harmonic orders. Also, restoration of the LB voltage amplitude and microgrid frequency to the rated values is considered.

The proposed hierarchical control scheme consists of two levels. The primary control comprises local controllers that control the output voltage of each DG in order to achieve the above-mentioned control functions and provide proper sharing of fundamental and non-fundamental powers among the microgrid DGs. The secondary control is performed by a centralized controller that sends proper reference signals to each of the DGs in order to reduce the voltage harmonic distortion to the required level and restore the LB voltage amplitude and microgrid frequency. Thus, by using this unique control system, high performance in terms of power quality can be achieved.

On the other hand, in order to share the nonlinear load among the DGs, fixed virtual resistances at harmonic frequencies can be used [12], [13]. Using fixed resistance may be ineffective in severely asymmetrical grids. Thus, the present paper proposes to adaptively set the virtual resistance value according to the nonlinear load supplied by the DG.

II. MICROGRID HIERARCHICAL CONTROL SCHEME

The structure of the proposed hierarchical control scheme applied to a general islanded microgrid is depicted in Fig. 1. The microgrid comprises of DGs and distributed loads (DLs). $Z_{\ell i}$ $(i=1,2,\ldots,n)$ and Z_j $(j=1,2,\ldots,m)$ represent the tie line impedance of DG_i and DL_j, respectively.

The secondary controller can be far from DGs and LB. Thus, as shown in Fig. 1, LB voltage and microgrid frequency information are sent to this controller by means of low bandwidth communication (*LBC*). In order to ensure that *LBC* is sufficient, the transmitted data should consist of approximately dc signals. Hence, before transmission, the LB voltage data are transformed to *dq* coordinates.

As shown in Fig. 1, for extraction of the LB voltage fundamental component and main harmonics (5^{th} and 7^{th}), at first, the measured LB voltage (v_{abc}) is transformed to *dq* (synchronous) reference frames rotating at ω, -5ω, and 7ω, respectively. ω is the system angular frequency estimated by a phase-locked loop (*PLL*). Afterwards, three second order low pass filters (*LPF*) with the cut-off

frequency of 5Hz are used to extract v_{dq}^{1}, v_{dq}^{5}, and v_{dq}^{7} which are the *dq* components at fundamental, 5th and 7th harmonic frequencies, respectively. The second order filters are applied; since, the first order ones cannot provide acceptable performance.

On the other hand, as seen in Fig. 1, *"Harmonic Compensation References"* (HCR_{dq}^{5} and HCR_{dq}^{7}: for 5th and 7th harmonics, respectively) which are also in *dq* frame are generated by the secondary controller and sent to the DGs local controllers which constitute the primary control level. Then, these references are transformed to *αβ* (stationary) frame and added as the references for the voltage controller, as shown in Fig. 2. The rotation angles of transformations are set to $-5\cdot\phi^{*}$ and $7\cdot\phi^{*}$ for the 5th and 7th harmonics, respectively. ϕ^{*} is the DG voltage reference phase angle which is generated by the active power droop controller as explained in Subsection IV-A.

Also, voltage amplitude and frequency restoration reference signals (E_{res} and ω_{res}, respectively) are generated by the secondary controller and then transmitted to the local controllers of all DGs. E_{res} is fed to the DG reactive power droop controller, as shown in Fig. 2. This way, LB fundamental voltage drop caused by reactive power droop controller, output impedance of the DG and impedance of tie line between DG and LB can be compensated. ω_{res} is the input of active power droop controller and is used to compensate the frequency drop caused by this controller (Subsection IV-A). The details about the generation of reference signals by the secondary controller are provided in the next Section.

III. Secondary Control Level

The block diagram of the central secondary controller is shown in Fig. 3. As can be seen in the "*Harmonics Compensation*" block, v_{dq}^{1}, v_{dq}^{5}, and v_{dq}^{7} are used to calculate 5th and 7th order harmonic distortions (HD_5 and HD_7, respectively). Then, the calculated values are compared with the reference ones (HD_5^{*} and HD_7^{*}, respectively). The errors are fed to the proportional-integral (PI) controllers. Afterwards, the outputs of these controllers are multiplied by v_{dq}^{5} and v_{dq}^{7} to generate HCR_{dq}^{5} and HCR_{dq}^{7}, respectively. If any of the harmonic distortions is less than the reference value, the respective deadband block prevents the increase of the distortion by the PI controller.

On the other hand, as shown in the "*Amplitude Restoration*" block of Fig. 3, amplitude of v_{dq}^{1} is compared with the rated amplitude ($E_{0,dq}=230\sqrt{3}$ in *dq* frame, equal to peak value of $230\sqrt{2}$ in *abc* frame) and E_{res} is generated using a PI controller. Also, as seen in "*Frequency Restoration*" block, the estimated ω is compared with the rated angular frequency (ω_0=100π). Then, the error is fed to a PI controller and ω_{res} is generated.

IV. DG Local Control System

The structure of each DG power stage and local controller is shown in Fig. 2. The power stage consists of a DC prime-mover, an interface inverter and a LC filter. The local controllers are designed in *αβ* reference frame; thus, the Clarke transformations are used to transform the variables between *abc* and *αβ* coordinates. More details about the local controller are presented in the following Subsections.

A. Calculation and Control of Fundamental Powers

Assuming mainly inductive grid and by considering the action of secondary controller, the following droop characteristics are applied to share the fundamental frequency powers among the DGs of an islanded microgrid:

$$\phi^{*}=(\phi_0+\int\omega_{res}dt)-(m_P P+m_I\int Pdt) \quad (1)$$

$$E^{*}=(E_0+E_{res})-n_P Q \quad (2)$$

where E_0 and ϕ_0 represent the rated voltage amplitude and phase angle ($\phi_0=\int\omega_0 dt=\omega_0 t$); P and Q are the fundamental active and reactive powers; m_P and m_I are proportional and integral coefficients for active power control; n_P is the proportional coefficient of reactive power controller; finally, E^{*} and ϕ^{*} represent the reference values of DG voltage amplitude and phase angle.

Power calculation details and more explanation regarding power control are presented in [7]-[9].

B. Voltage and Current Controllers

Due to the difficulties of using PI controllers to track non-dc variables, proportional-resonant (PR) controllers are usually preferred in the stationary reference frame [14]. In this paper, PR voltage and current controllers are as follow:

$$G_V(s)=k_{pV}+\sum_{k=1,5,7}\frac{2k_{rV_k}\cdot\omega_{cV_k}\cdot s}{s^2+2\cdot\omega_{cV_k}\cdot s+\left(k\cdot\omega_0\right)^2} \quad (3)$$

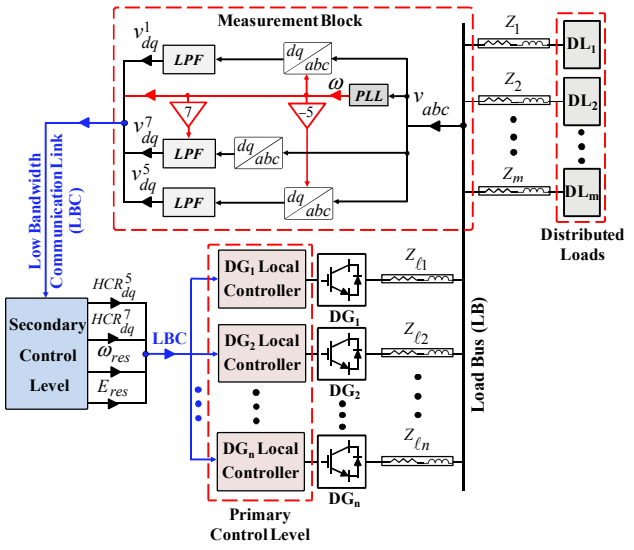

Fig. 1. Block diagram of hierarchical control scheme.

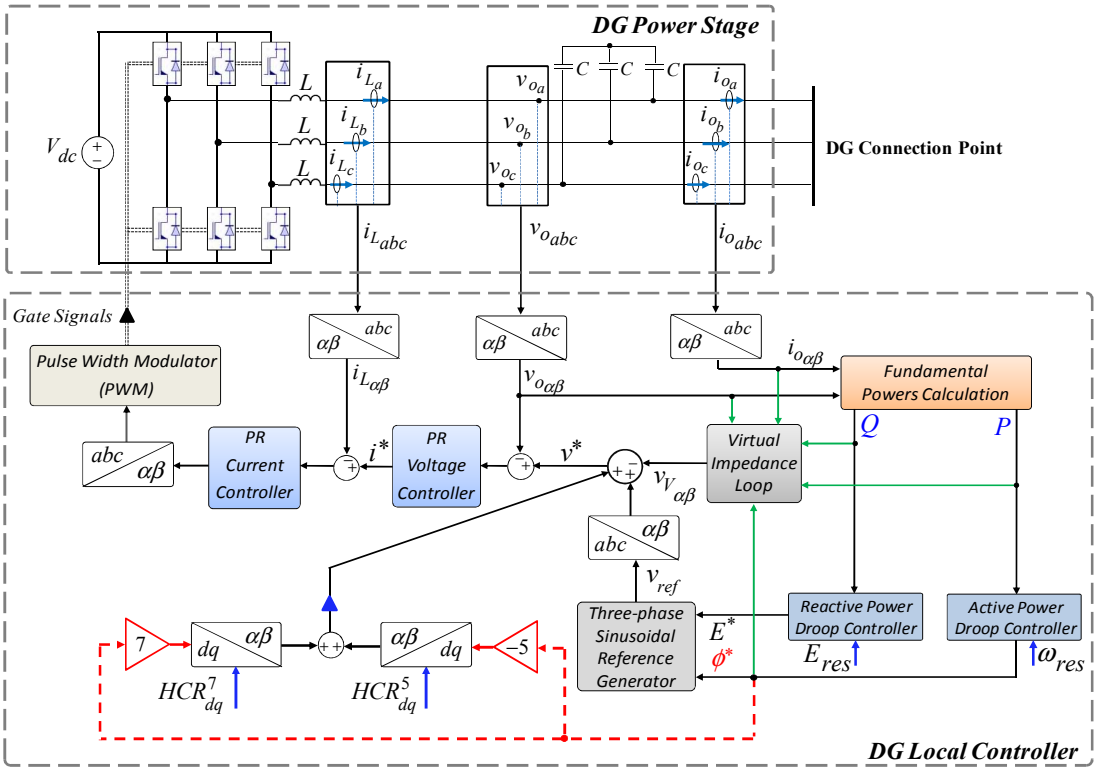

Fig. 2. DG power stage and local controller.

$$G_I(s) = k_{pI} + \sum_{k=1,5,7} \frac{2k_{rI_k} \cdot \omega_{cI_k} \cdot s}{s^2 + 2 \cdot \omega_{cI_k} \cdot s + \left(k \cdot \omega_0\right)^2} \quad (4)$$

where k_{pV} (k_{pI}) and k_{rV_k} (k_{rI_k}) are the proportional and k^{th} harmonic resonant coefficients of the voltage (current) controller, respectively. ω_{cV_k} and ω_{cI_k} represent the voltage and current controllers cut-off frequencies at k^{th} harmonic, respectively.

C. Virtual Impedance Loop

The basic structure of virtual impedance is presented in [15]. Here, this structure is extended as shown in Fig. 4, where R_v and L_v are the fundamental frequency virtual resistance and inductance, respectively, and $R_{v,harm}$ is the virtual resistance at 5th and 7th harmonics as the main harmonic orders.

Addition of the fundamental frequency virtual resistance contributes toward damping the system oscillations [12]. Also, the virtual inductance is considered at fundamental frequency to make the grid inductive enough and improve the power control stability [13].

Harmonic virtual resistance is included in order to improve the sharing of non-fundamental (harmonic) apparent power (S_n) among the microgrid DGs. As shown in Fig. 4, $R_{v,harm}$ is set in proportion to S_n using the following boost characteristic:

$$R_{v,harm} = K_v \cdot S_n \quad (5)$$

where K_v is a small positive constant which determines the slope of the boost characteristic.

Thus, by increase of the non-fundamental power, $R_{v,harm}$ increases. The increment of $R_{v,harm}$ prevents the excessive nonlinear load supply by individual DGs. This way, a proper sharing can be achieved.

The details of S_n calculation are presented in Fig. 4 [16], where S_f, THD_I and THD_V are the fundamental apparent power and total harmonic distortions of current and voltage, respectively. *THD* values are calculated as shown in *(THD)² Calculation*" block of Fig. 4 [17], where, $i^1_{o_{dq}}$ and $i^{os}_{o_{dq}}$ represent the fundamental and oscillatory parts of output current in *dq* coordinates, respectively. The same method is applied for $(THD_V)^2$ calculation.

V. Simulation Results

The two-DG islanded microgrid of Fig. 5 is considered as the test system. Switching frequency of the DGs inverters is 10 kHz. A diode rectifier is considered as the nonlinear load. A star-connected linear load (Z_L) is also connected to LB. The microgrid is rated at 230 V (rms of phase voltage) and 50Hz.

Power stage and control system parameters are listed in Tables I-III. As can be seen in Table I, $Z_{\ell 1} = 2Z_{\ell 2}$ is considered double of $Z_{\ell 2}$ in order to simulate asymmetrical DG tie lines.

Four simulation steps are considered:

- Step0($0 \le t < 2s$): DGs operate with only fundamental virtual impedance and secondary control is not acting.
- Step1($2 \le t < 3.5s$): Harmonic virtual resistance is added.
- Step2($3.5 \le t < 5s$): Secondary control for frequency and voltage amplitude restoration is activated.
- Step3($5 \le t < 6.5s$): Secondary control for harmonic compensation is activated. ($HD_5^* = HD_7^* = 0.5\%$).

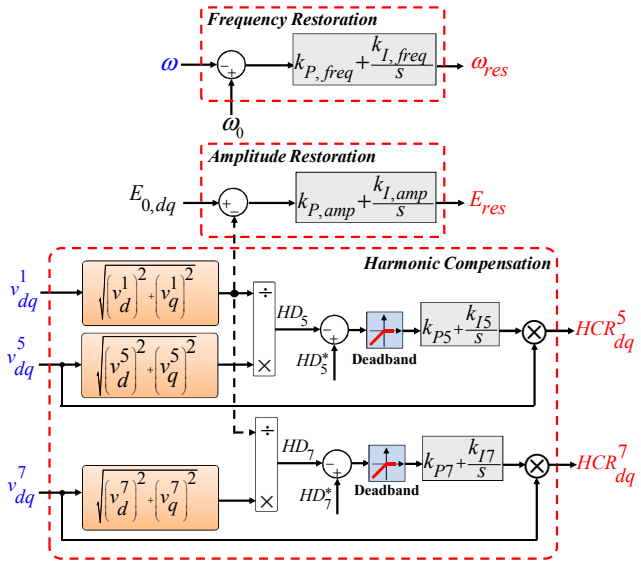

Fig. 3. Block diagram of secondary controller.

As shown in Figs. 6(a) and 6(b), HD_5^* and HD_7^* of the DGs output voltage are very small before adding the harmonic virtual resistance. This fact reveals the effectiveness of the local controllers in tracking the reference voltage. But, LB harmonic distortion is noticeable due to harmonic voltage drop on the tie lines. Fig. 7(a) shows the LB harmonic distortion clearly.

After addition of the harmonic virtual resistance at t=2s, the distortion of the DGs output voltage increase as shown in Fig. 6. Consequently, the LB voltage becomes more distorted as can be seen in Fig. 7(b). As explained earlier addition of the harmonic virtual resistance contributes toward improving the non-fundamental power sharing as presented in Fig. 8(a). Also, fundamental powers are affected by $R_{v,harm}$ addition, as shown in Figs. 8(b) and 8(c). In fact, due to the nonlinear load nature, the harmonic and fundamental frequency components cannot be assumed completely decoupled. However, it can be observed that the fundamental powers are properly shared during the whole under-study interval, in spite of the asymmetrical tie line impedances. It demonstrates the effectiveness of the droop controllers. The coupling between harmonic and fundamental frequency can also be observed in Fig. 9 as the change of LB fundamental voltage magnitude and the system frequency in $2 \le t < 3.5s$ interval.

In the next simulation step, restoration of LB voltage amplitude and the microgrid frequency is activated at t=3.5s. As shown in Fig. 9, amplitude and frequency are restored to the rated values, properly. The amplitude restoration can also be noticed from Fig. 7(c).

TABLE I
POWER STAGE PARAMETERS

DG Prime-Mover	LC Filter Inductance	LC Filter Capacitance	Nonlinear Load Tie Line
$V_{dc}\,(V)$	$L\,(mH)$	$C\,(\mu F)$	$Z\,(\Omega)$
650	1.8	25	0.1+j0.56
DG_1/DG_2 Tie Line	Nonlinear Load		Linear Load
$Z_{\ell 1}\,(\Omega) / Z_{\ell 2}\,(\Omega)$	$C_{NL}\,(\mu F) / R_{NL}\,(\Omega) / L_{NL}\,(mH)$		$Z_L\,(\Omega)$
0.2+j1.12/0.1+j0.56	235/100/0.084		50+j6.28

TABLE II
DG LOCAL CONTROLLER PARAMETERS

Power Controllers			Virtual Impedance		
m_P	m_I	n_P	$R_v\,(\Omega)$	$L_v\,(mH)$	K_v
2×10^{-5}	2×10^{-4}	0.1	1	4	0.015
Voltage Controller						
k_{pV}	k_{rV_1}	k_{rV_5}	k_{rV_7}	ω_{cV1}	ω_{cV5}	ω_{cV7}
1	100	50	50	2	2	2
Current Controller						
k_{pI}	k_{rI_1}	k_{rI_5}	k_{rI_7}	ω_{cI1}	ω_{cI5}	ω_{cI7}
10	1000	100	100	2	2	2

TABLE III
SECONDARY CONTROLLER PARAMETERS

Frequency Restoration		Amplitude Restoration	
$k_{P,freq}$	$k_{I,freq}$	$k_{P,amp}$	$k_{I,amp}$
0.02	0.15	0.2	0.25
5th Harmonic Compensation		7th Harmonic Compensation	
k_{P5}	k_{I5}	k_{P7}	k_{I7}
0.5	20	0.5	30

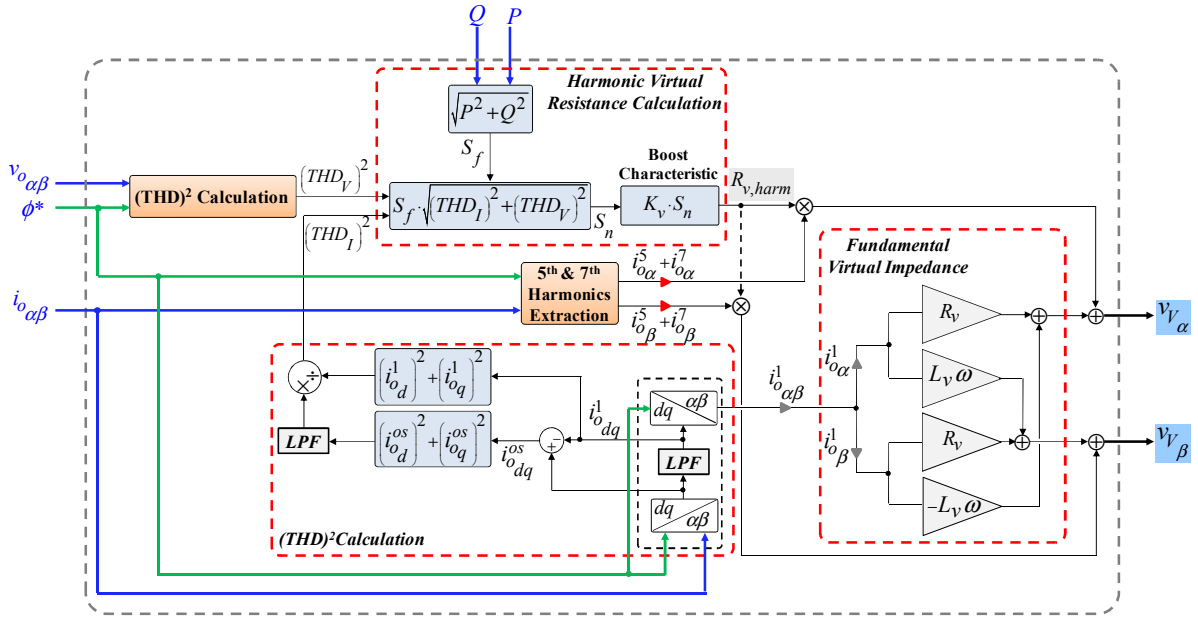

Fig. 4. Block diagram of virtual impedance

As expected, the restoration leads to the increase of the fundamental powers as seen in Figs. 8(b) and 8(c). Also, due to the increase of nonlinear load terminal voltage, more non-fundamental power should be supplied by the DGs as can be observed in Fig. 8(a).

Finally, harmonic compensation is activated at t=5s. As seen in Fig. 6(a) and 6(b), HD_5 and HD_7 track the reference values, properly. It leads to the considerable improvement of LB voltage quality as shown in Fig. 7(d). In fact, the harmonic compensation is achieved by the change of DGs output voltage distortion as depicted in Figs. 6(a) and 6(b). Note that DG_2 distortion changes with a behavior similar to the LB distortion, because, DG_2 tie line impedance is relatively low and thus, this DG and LB are electrically near.

As seen in Fig. 8(a), harmonic compensation requires noticeable increase of the non-fundamental power injection of the DGs. Also, due to the aforementioned coupling, activation of harmonic compensation results in change of fundamental powers according to Figs. 8(b) and 8(c). Furthermore, as can be observed in Fig. 9, harmonic compensation induces small deviations in LB voltage amplitude and the frequency. The deviations are properly damped by the amplitude and frequency controllers.

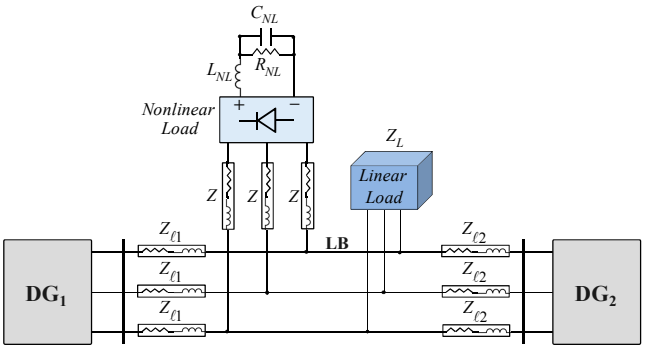

Fig. 5. Test system for simulation studies.

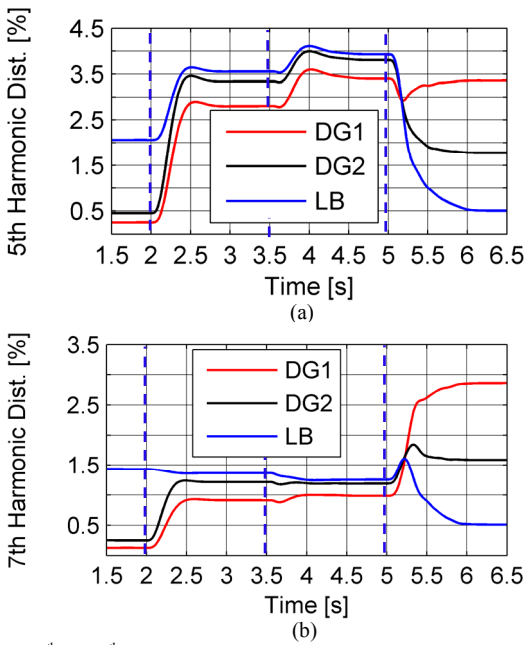

Fig. 6. 5th and 7th harmonic distrotion at LB and DGs terminal: (a) 5th harmonic, (b) 7th harmonic

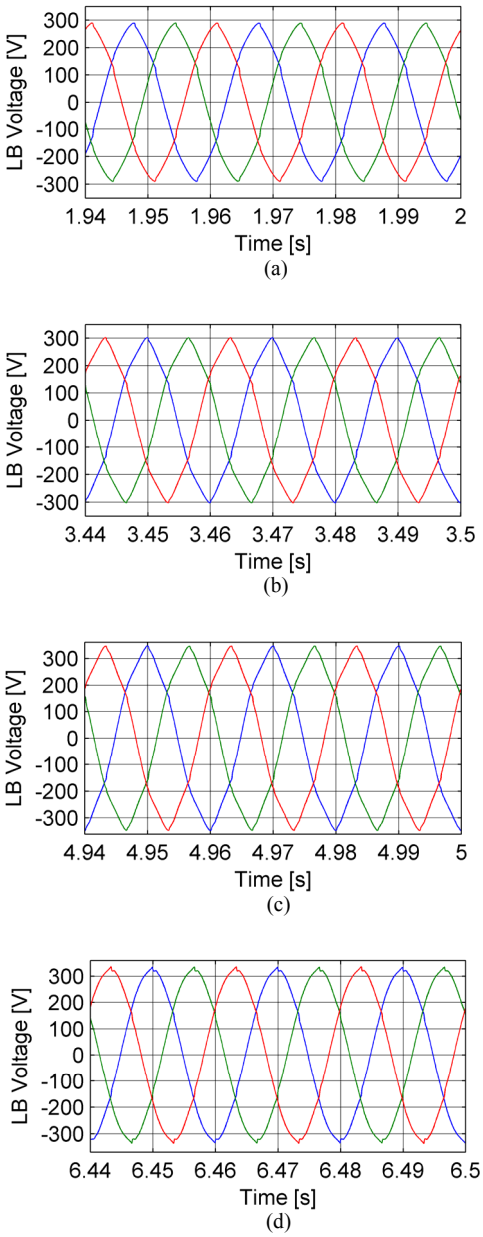

Fig. 7. Three-phase LB voltages at different simulation steps. (a) Step0, (b) Step1, (c) Step2, (d) Step3

VI. CONCLUSIONS

A hierarchical control structure consisting of primary and secondary levels is proposed for islanded microgrids. The secondary level controls selective compensation of LB voltage harmonics and restoration of LB voltage amplitude and system frequency to the rated values. These functions are provided by sending proper control signals to the primary level. A novel virtual impedance scheme is proposed to improve nonlinear load sharing. The presented simulation results show that the LB voltage quality is enhanced significantly as a result of compensation, while, fundamental and non-fundamental powers are shared, properly.

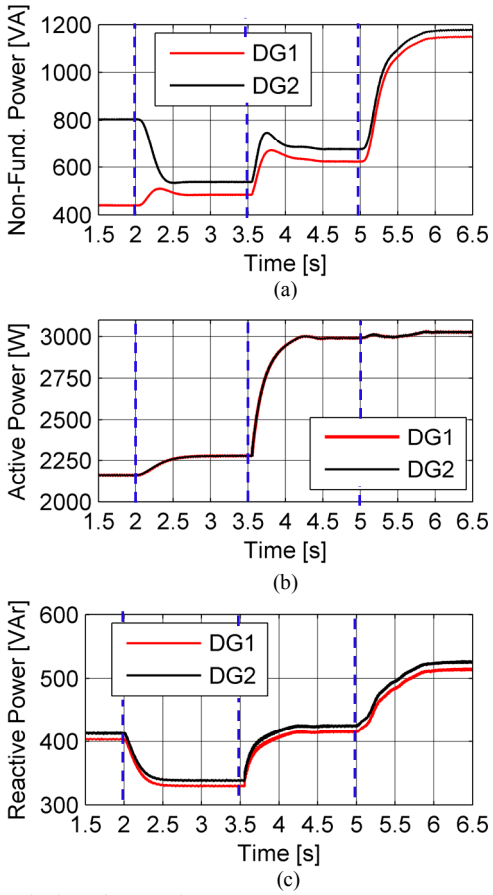

Fig. 8. Sharing of powers between DGs
(a) non-fundamental power, (b) active power, (c) reactive power,

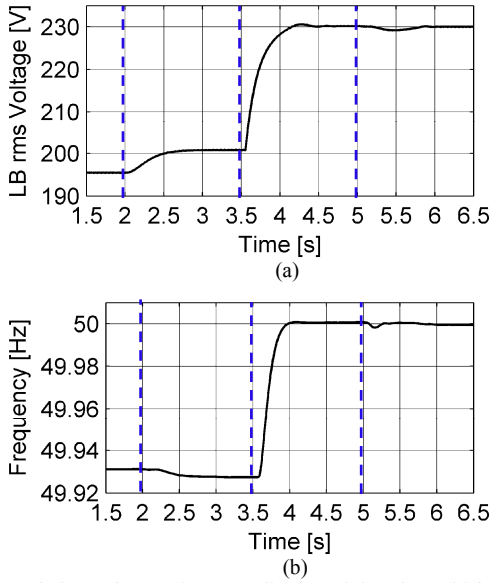

Fig. 9. Variations of: (a) voltage amplitude and (b) microgrid frequency

REFERENCES

[1] *IEEE Guide for Design, Operation, and Integration of Distributed Resource Island Systems with Electric Power Systems*, IEEE Standard 1547.4-2011, 2011.

[2] T. Takeshita, and N. Matsui, "Current waveform control of PWM converter system for harmonic suppression on distribution system," *IEEE Trans. Ind. Elec.*, vol. 50, no. 6, pp. 1134-1139, Dec. 2003.

[3] N. Pogaku, and T. C. Green, "Harmonic mitigation throughout a distribution system: a distributed-generator-based solution," *IEE Proc.-Gener. Transm. Distrib.*, vol. 153, no. 3, pp. 350-358, May 2006.

[4] M. Prodanovic, K. D. Brabandere, J. V. Keybus, T. C. Green, and J. Driesen, "Harmonic and reactive power compensation as ancillary services in inverter-based distributed generation," *IET Gener. Transm. Distrib.*, vol. 1, no. 3, pp. 432-438, May 2007.

[5] J. He, Y. W. Li, and M. S. Munir, "A flexible harmonic control approach through voltage controlled DG-grid interfacing converters," *IEEE Trans. Ind. Elec.*, Early Access, Apr. 2011.

[6] T. L. Lee, and P. T. Cheng, "Design of a new cooperative harmonic filtering strategy for distributed generation interface converters in an islanding network," *IEEE Trans. Pow. Elec.*, vol. 22, no. 5, pp. 1919-1927, Sept. 2007.

[7] M. Savaghebi, J. M. Guerrero, A. Jalilian, and J. C. Vasquez, "Selective compensation of voltage harmonics in a grid-connected microgrid," in *Proc. 2011 Electrimacs Conf.* , pp.1-6.

[8] J. M. Guerrero, J. C. Vasquez, J. Matas, L. G. de Vicuña, and M. Castilla, "Hierarchical control of droop-controlled AC and DC microgrids—a general approach toward standardization," *IEEE Trans. Ind. Elec.*, vol. 58, no. 1, pp. 158-172, Jan. 2011.

[9] J. C. Vasquez, J. M. Guerrero, M. Savaghebi, and R. Teodorescu, "Modeling, analysis, and design of stationary reference frame droop controlled parallel three-phase voltage source inverters," in *Proc 2011, 8th Int. Conf. on Pow. Elec. (ICPE)*, pp. 272-279.

[10] J. P. Lopes, C. Moreira, and A. G. Madureira, "Defining control strategies for microgrids islanded operation," *IEEE Trans. Pow. Sys.*, vol. 21, no. 2, pp. 916-924, May 2006.

[11] A. Mehrizi-Sani and R. Iravani, "Potential-function based control of a microgrid in islanded and grid-connected modes," *IEEE Trans. Pow. Sys.*, vol. 25, no. 4, pp. 1883-1891, Nov. 2010.

[12] J. M. Guerrero, J. Matas and L. G. de Vicuña, M. Castilla, and J. Miret, "Decentralized control for parallel operation of distributed generation inverters using resistive output impedance," *IEEE Trans. Ind. Elec.*, vol. 54, no. 2, pp. 994-1004, Apr. 2007.

[13] J. M. Guerrero, L. G. Vicuna, J. Matas, M. Castilla, and J. Miret, "Output impedance design of parallel-connected UPS inverters with wireless load sharing control," *IEEE Trans. Ind. Elec.*, vol. 52, no. 4, pp. 1126-1135, Aug. 2005.

[14] F. Blaabjerg, R. Teodorescu, M. Liserre and A. V. Timbus, "Overview of control and grid synchronization for distributed power generation systems," *IEEE Trans. Ind. Electron.*, vol. 53, no. 5, pp. 1398-1409, Oct. 2006.

[15] J. He, and Y. W. Li "Analysis and design of interfacing inverter output virtual impedance in a low voltage microgrid," in *Proc 2010, Energy Conv. Cong. and Exp. (ECCE)*, pp. 2857–2864.

[16] *IEEE Standard Definitions for the Measurement of Electric Power Quantities Under Sinusoidal, Nonsinusoidal, Balanced, or Unbalanced Conditions*, IEEE Standard 1459-2010, 2010.

[17] P. Jintakosonwit, H. Akagi, H. Fujita, and S. Ogasawara, "Implementation and performance of automatic gain adjustment in a shunt active filter for harmonic damping throughout a power distribution system," *IEEE Trans. Pow. Elec.*, vol. 17, no. 3, pp. 438-447, Mar. 2002.